Idealized Study of Seasonal Dynamics in the Southern Ocean

Takaya Uchida[1], Ryan Abernathey[1], Shafer Smith[2] and Dhruv Balwada[2]

1: Lamont-Doherty Earth Observatory, Columbia University, 2: Center for Atmosphere Ocean Science, New York University

Objectives

We examine the seasonal dynamics in a eddy permitting simulation configured for the Southern Ocean. Seasonally resolved wavenumber power spectra are calculated for eddy kinetic energy (EKE). The EKE spectra consistently show higher power at small scales during winter throughout the domain. Our study looks into:

- Seasonality of EKE in the Southern Ocean.
- Seasonality of baroclinic instability and isopycnal slopes.

Introduction

In this study, we investigate seasonal variability in wavenumber power spectra for eddy kinetic energy (EKE) in an ocean model configured for the Southern Ocean. SSH and velocity fields through geostrophic balance are observable through remote sensing, albeit with significant noise and sampling issues, and a numerical simulation study provides a useful test bed for future work on satellite observations by the Surface Water Ocean Topography (SWOT) satellite [1], expected to launch in 2021. According to the criteria of [2] , the 10 km and 5 km-resolution of our simulation is in the range of mesoscale permitting to resolving. Although this is rather coarse for a regional model, it allows for a direct comparison with global climate models that have roughly 0.1° resolution [3]. Additionally, because of its resolution and dynamical limitations, the analysis of such simulations serves as an experiment into the mechanisms which can drive seasonality.

Model description

The code solves the hydrostatic Boussinesq equations in Cartesian coordinates on the β plane using the Massachusetts Institute of Technology general circulation model (MITgcm). The model setup is similar to the flat-bottom case in [4] with seasonal forcings (Figs. 1,2). Since the model domain is a channel, it is configured to represent the *zero-residual* overturning circulation regime. The MITgcm run has:

- Level-coordinate ocean GCM with three-dimensional primitive equations.
- Subgrid scale horizontal mixing is parameterized using the Leith scheme [5].
- The vertical diffusion depends on the K-profile parameterization (KPP) of [6].
- The 10 km run has 40 vertical layers (mesoscale permitting) and 5 km run 76 layers (mesoscale resolving).
- No salinity stepping.
- The first deformation wavelength ($\lambda_d = 2\pi R_d$) is around 100 km.
- The model was spun up for 240 years with monthly varying SST relaxation and wind stress forcing.

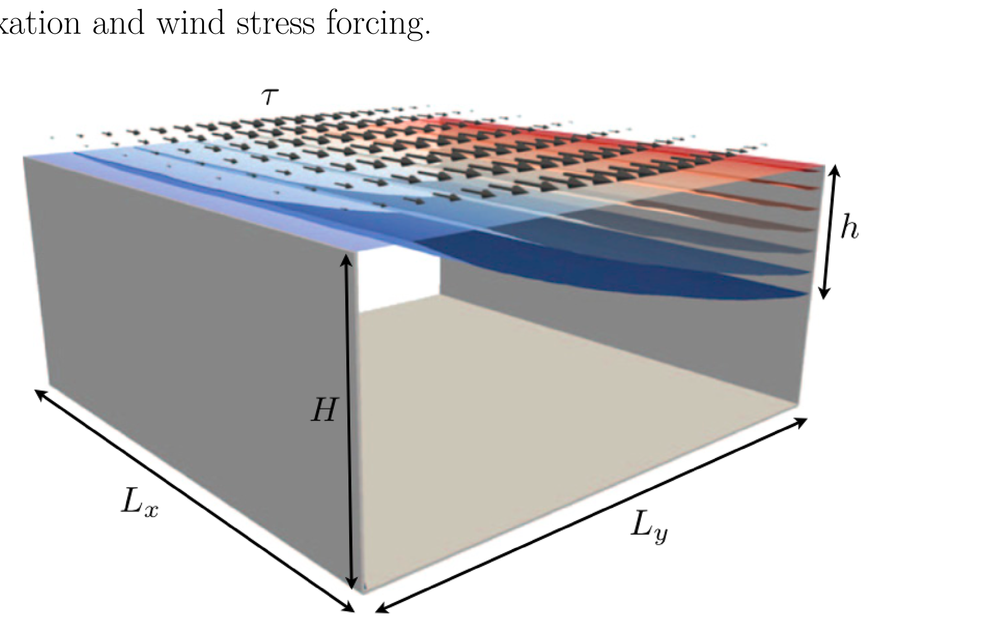

Figure 1: The channel model domain with the size of $L_x = 1000$ km $\times$ $L_y = 2000$ km $\times$ $H = 2985$ m.

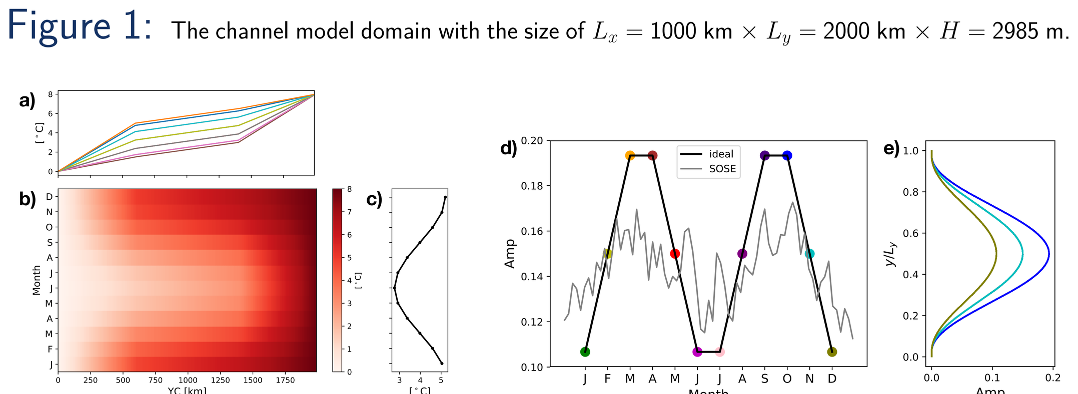

Figure 2: Monthly SST and wind stress forcing.

Climatological outputs

We see that the month at which domain averaged SST takes its minimum and maximum are roughly in phase with the Southern Ocean State Estimate (SOSE [7]).

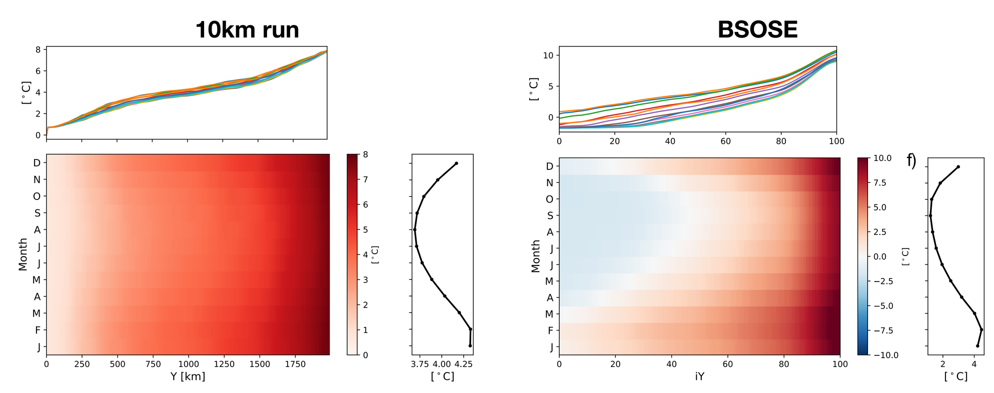

Figure 3: The SST monthly climatology from our channel run (left) and SOSE (right).

Figure 4 shows the zonally averaged climatological buoyancy frequency, residual overturning stream function, mixed-layer (ML) depth, and diagnosed surface heat flux. The residual overturning circulation is smaller than 1 Sv everywhere in the domain as expected.

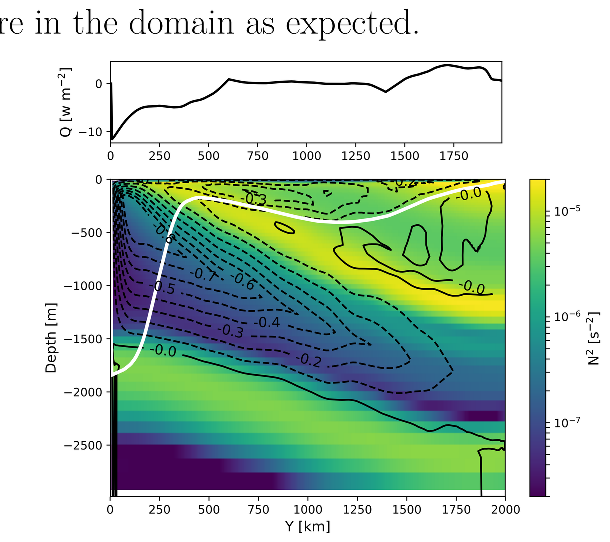

Figure 4: The top panel shows the surface heat flux (Q). The bottom panel shows the buoyancy frequency (N^2; in color), residual overturning stream function (ψ_{res}; black) and the MLD (white).

Local mixed-layer depth maxima

Figure 4 shows the zonally averaged climatological buoyancy frequency, residual overturning stream function, mixed-layer (ML) depth, and diagnosed surface heat flux. The residual overturning circulation is smaller than 1 Sv everywhere in the domain and our run captures the local maxima of ML depth, a prominant feature along the ACC front (Fig. 5).

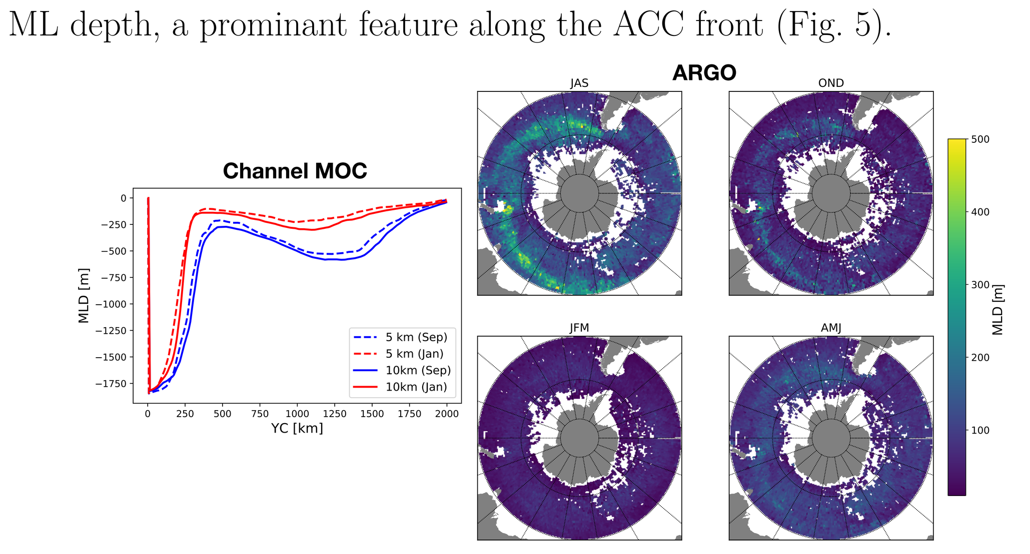

Figure 5: The monthly climatological zonal-mean of MLD in our channel runs (left) and seasonal climatology of MLD from ARGO floats (right).

We see that the MLD is more or less equivalent to the diabatic layer, i.e. layers where isentropes outcrop at the surface, which is shown where the percentage is lower than unity in Fig. 6.

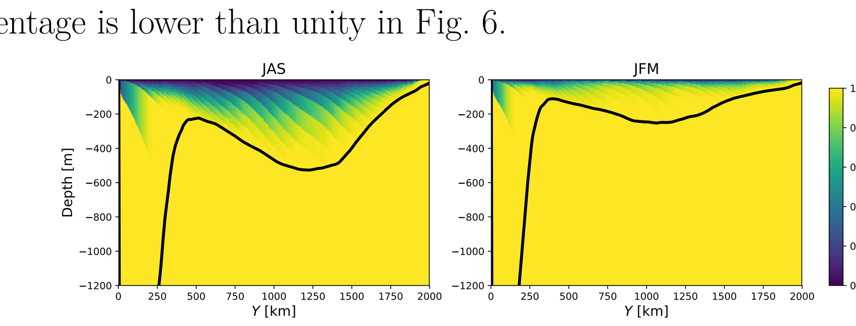

Figure 6: The percentage that the isentrope outcrops is shown in color and MLD in the black solid line for JAS (left) and JFM (right).

Important Result

EKE at scales smaller than 100 km showed coherent seasonality across the domain, consistent with the seasonality of baroclinic conversion rates ($\overline{w'b'}$) and in phase with the buoyancy forcing.

EKE wavenumber spectra

Figure 7 shows the longitudinal wavenumber spectra of surface EKE $(\hat{\overline{u'}}^2 + \hat{\overline{v'}}^2)/2$ where the primes denote the deviation from the *seasonal climatology* and zonal mean and the overline denotes a temporal and meridional mean) along with the monthly climatology of EKE, baroclinic energy conversion rates ($\overline{w'b'}$) at z=100 m, zonal wind stress (τ) and surface heat flux (Q). EKE is higher during wintertime compared to summertime at spatial scales of 100 km and smaller, consistent with our findings in ([3], Fig. 8).

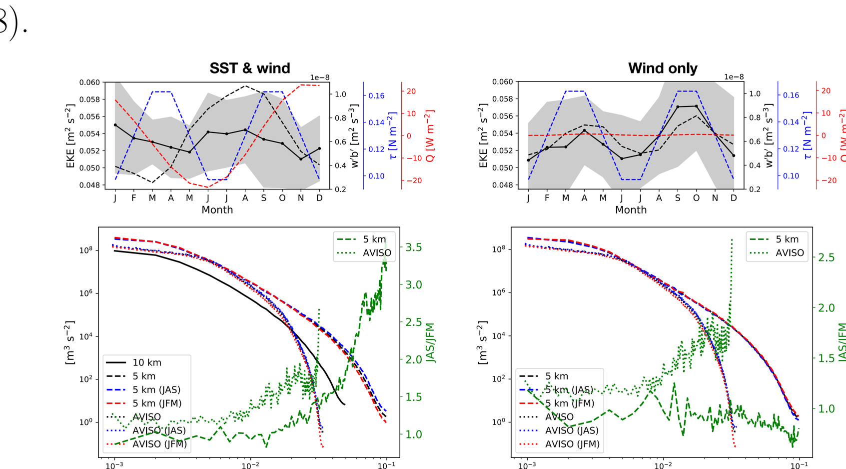

Figure 7: The monthly EKE (solid black) and $w'b'$ (dashed black) averaged between Y=600-1400km are shown (top panels). EKE spectra for both monthly-varying SST and wind stress forcing (left), and monthly-varying wind stress but constant SST forcing (right) are shown on the bottom panels.

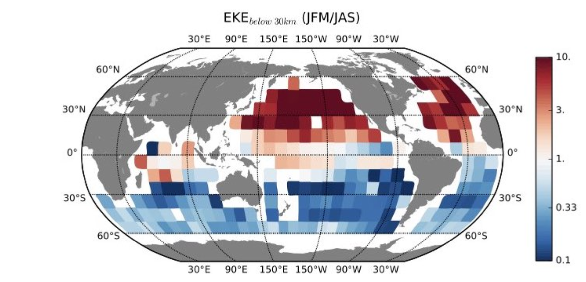

Figure 8: Seasonality of surface EKE isotropic wavenumber spectra below 30 km from a 0.1° CESM

Baroclinic energy conversion

The seasonality of $\overline{w'b'}$ is shown in Fig. 9. It is interesting to note that the seasonality of energy conversion is largest within the KPP boundary layer.

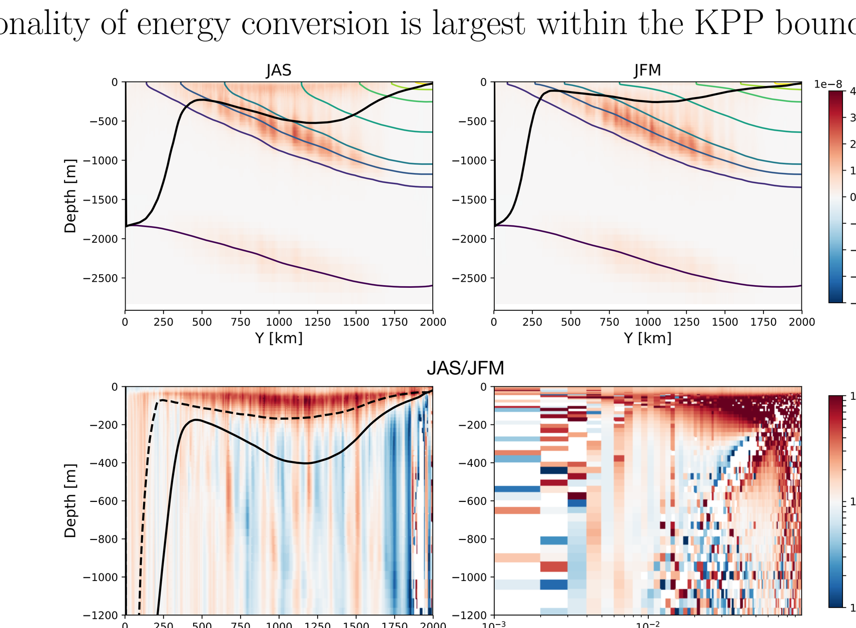

Figure 9: The APE conversion rate for JAS and JFM (top) and their ratio (bottom). The isentropes are shown in colored contours and the black solid line shows the MLD and dashed line the 99 percentile of KPP boundary layer depth, i.e. the depth over which KPP mixing is enhanced.

We see that the seasonality is consistent in the Southern Ocean in a CESM run shown by (Fig. 10, [3]).

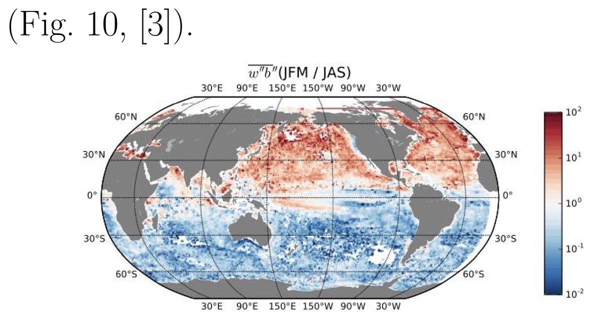

Figure 10: The APE conversion rate in the top 100 m from a 0.1° CESM run. The double primes denote submonthly variability.

Baroclinic instability

We show the seasonality of baroclinic instability growth rates of the model in Fig. 11 with the background profiles of zonal-mean seasonal climatological buoyancy frequency and geostrophic velocities at Y=1250 km. [3] showed that the large growth rates near the Nyquist wavelength during winter are due to the reduced stratification in the ML. The local maximum around 200 km coincide with the scale at which the Eady growth rate calculated over the full-depth profile takes its maximum. The seasonality in *deep* baroclinic instability likely come from the seasonality in isopycnal slopes shown in the section below.

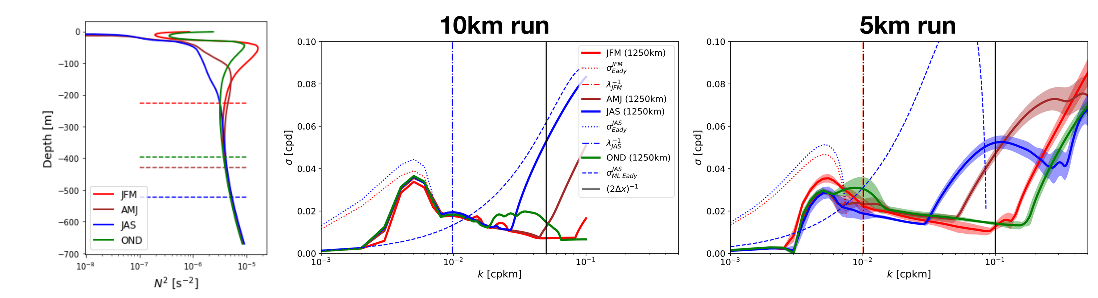

Figure 11: The Nyquist Frequency and MLD are shown on the left. Growth rate of baroclinic instability plotted against inverse wavelength. The ML and full-depth Eady growth rates are shown in dotted and dashed lines respectively. The seasonal deformation wavelength and Nyquist wavelength are shown in dot-dashed lines.

Isopycnal slope

The monthly transition of the isentropic slopes belwo the diabatic layer are shown in Fig. 12. They lag the surface wind stress by $\sim$2 months, consistent with results shown by [8] . This change in isentropic slopes are likely the cause for seasonality in the *deep* baroclinic instability (i.e. local maximum and minimum in the slopes during February and September respectively).

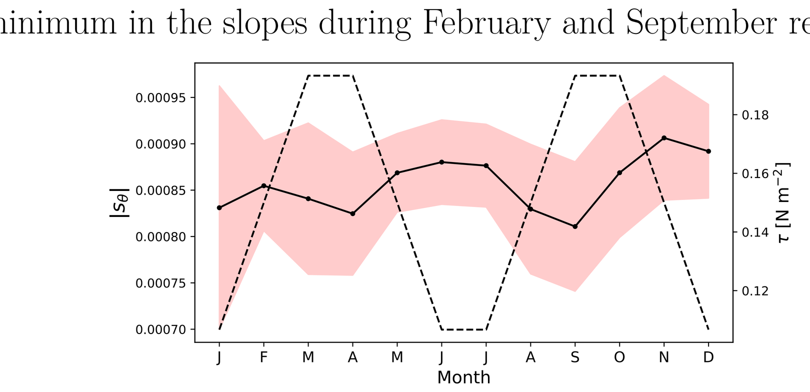

Figure 12: The isopycnal slopes (solid black line), its standard deviation (red shading) and the amplitude of surface wind stress (dashed black line).

Conclusion

Evidence from diagnostics of baroclinic APE conversion rates and linear quasi-geostrophic stability analysis indicate that seasonally varying mixed-layer instability [9] is responsible for the EKE seasonality at scales below 100 km. Austral winter (JAS) and summer (JFM) are in the same phase of wind stress seasonality so EKE and ML APE conversion is in phase with the surface diabatic forcing. Comparing our results to a run with constant SST relaxation but monthly varying wind stress showed that seasonally varying buoyancy forcing is necessary in getting the seasonality in phase with AVISO.

The isentropic slopes below the diabatic layer lag the wind stress forcing by $\sim$2 months, which is expected from Ekman pumping ([8]).

In future studies, we plan to have a run with submesoscale resolving resolution to compare with our results shown here and along-track satellite observations, and couple our runs to the Darwin biogeochemical model [10] to see how seasonality in (sub)mesoscale turbulence affects primary production in the Southern Ocean.

Contact Information

- Website: https://roxyboy.github.io
- Email: takaya@ldeo.columbia.edu